International Journal of Biochemistry and Cell Biology 112 (2019) 114–122

Contents lists available at ScienceDirect

International Journal of Biochemistry and Cell Biology

journal homepage: www.elsevier.com/locate/biocel

Microvesicles derived from human Wharton's Jelly mesenchymal stem cells ameliorate acute lung injury partly mediated by hepatocyte growth factor

Wenxia Chen[a], Shumin Wang[b], Hengjie Xiang[a], Jie Liu[c], Yudan Zhang[b], Shasha Zhou[b], Tao Du[c,*], Lei Shan[c,*]

[a] Department of Pediatrics, The First Affiliated Hospital of Henan University of Traditional Chinese Medicine, Zhengzhou, China
[b] Department of Pediatrics, Henan University of Traditional Chinese Medicine, Zhengzhou, China
[c] Department of Urology, Henan Provincial People's Hospital, Zhengzhou, China

ARTICLE INFO

Keywords:
Acute lung injury
Hepatocyte growth factor
Mesenchymal stem cells
Microvesicles
PI3K/AKT/mTOR pathway

ABSTRACT

Several studies have highlighted the underlying role of mesenchymal stem cells microvesicles (MSC-MVs) in acute lung injury (ALI). Hepatocyte growth factor (HGF) derived from MSC-MVs is partly involved in their therapeutic effects; however, the detailed mechanism remains unclear. MVs were isolated from human Wharton's Jelly MSCs. The rat model of ALI was established by intratracheal instillation of bleomycin (BLM). A co-culture model of alveolar epithelial cells or pulmonary endothelial cells and MSC-MVs was utilized. Total protein content in bronchoalveolar lavage fluid (BALF) was determined by bicinchoninic acid method. White blood cell (WBC) and neutrophil in BALF were counted. ELISA was used for the determination of cytokines and HGF in BALF. Apoptosis was determined by TUNEL assay and Annexin V-FITC/PI staining as well as caspase-3 activity detection. HE and Masson staining of lung tissues was used for histopathology analysis. The expression of HGF and proteins involved in the PI3K/AKT/mTOR pathway were measured by quantitative Real-Time PCR (qRT-PCR) and western blotting. Treatment with MSC-MVs significantly inhibited BLM-induced apoptosis and fibrosis in lung tissues and PI3K/AKT/mTOR activation, which was reversed by HGF mRNA deficient MVs. Intriguingly, these effects were completely abrogated by PI3K inhibitor. The therapeutic effect of MSC-MVs in ALI was partly mediated through HGF mRNA.

1. Introduction

Acute lung injury (ALI) is a severe, life-threatening condition characterized by diffuse interstitial pulmonary edema caused by pulmonary capillary endothelial cell and alveolar epithelial cell injury, leading to acute hypoxic respiratory insufficiency or lung failure (Yuan et al., 2016). The pathogenesis of ALI is very complex. Thus, few therapeutic strategies for clinical ALI have emerged, and the current specific treatment options remain limited. Mesenchymal stem cells (MSCs) are a population of self-renewing and endogenous multipotent precursor cells which have the capacity to differentiate into osteocytes, chondrocytes, adipocytes, neurocytes, muscular cells and so on in specific conditions (Squillaro et al., 2016). In recent years, abundant studies provided strong evidence that MSCs administration could effectively improve recovery from ALI by reducing the impairment of alveolar fluid clearance and interacting with components of innate and adaptive immune systems (Chan et al., 2016; Ho et al., 2015). However, the specific mechanism underlying the therapeutic benefit of MSCs for ALI is not fully illuminated.

Several lines of evidence suggest that MSCs exert therapeutic effects through paracrine action, which may be accounted for, at least in part, by microvesicles (MVs) released from MSCs, resulting in a horizontal transfer of microRNA, mRNA and proteins. MVs play crucial roles in cell-to-cell communication as a key component of paracrine secretion (Biancone et al., 2012; Ratajczak et al., 2012). Indeed, MVs may directly stimulate target cells by receptor-mediated interactions or transfer from the cell of origin to various bioactive molecules including membrane receptors, proteins, mRNAs, microRNAs, and organelles (Camussi et al., 2010). Compelling evidence has delineated the therapeutic effects of MVs derived from MSCs on attenuating ALI (Monsel et al., 2016). However, the molecular mechanism by which MVs exerts protective effect on lung injury is largely unclear. Our previous studies have demonstrated that human umbilical cord MSCs (hUC-MSCs)-derived MVs delivered human HGF mRNA into injured rat tubular cells and translated it into HGF protein, while RNase treatment abrogated the therapeutic effect of MVs on acute kidney injury (AKI) (Du et al.,

* Corresponding authors at: Department of Urology, Henan Provincial People's Hospital, No. 7 Weiwu Road, Jinshui District, 450003, Zhengzhou, China.
E-mail addresses: lcg78032@163.com (T. Du), wwwdingpracht@foxmail.com (L. Shan).

https://doi.org/10.1016/j.biocel.2019.05.010
Received 29 January 2019; Received in revised form 23 April 2019; Accepted 13 May 2019
Available online 14 May 2019
1357-2725/

2013a,2013b; Ju et al., 2015). Given that anti-apoptosis and anti-fibrosis effect of MSC-MVs in AKI was partly through the transfer of HGF mRNA into injured cells, we hypothesized that HGF may also be involved in the therapeutic effect of MSC-MVs in ALI.

Recently, several researches have proposed that the hepatocyte growth factor (HGF)/c-Met signaling pathways are responsible for epithelial-mesenchymal transition (EMT) and angiogenesis in damaged lung tissues (Jiao et al., 2016). Activation of the downstream signaling components including PI3K/Akt/mTOR, ERK-MAPK and the JAK/STAT pathway is associated with increased invasion, proliferation, survival, and angiogenesis (Han et al., 2016; Jiao et al., 2016). It is noteworthy that the PI3K-Akt-mTOR signaling pathway is regarded as a promising therapeutic target for ALI (Meng et al., 2018).

Based on the above evidence, we thus speculated that hUC-MSCs-derived MVs might transfer HGF mRNA into alveolar epithelial cells and pulmonary vascular endothelial cells, which in turn activate the PI3K-Akt-mTOR signaling pathway, thereby alleviating ALI.

2. Materials and methods

2.1. Isolation and identification of hWJMSC-MVs

Fresh human umbilical cords were collected from newborn infants and stored at 4 °C in Hank's balanced salt solution, with the written consent of their parents. This experiment was approved by the Ethics Committee of Henan Provincial People's Hospital. The mesenchymal tissues were cut into 1 mm^3 pieces and suspended in low-glucose Dulbecco's modified Eagle's medium (DMEM; Life Technologies, Carlsbad, CA, USA) supplemented with 10% fetal bovine serum (FBS; Gibco, Carlsbad, CA, USA). The medium was replaced every 48 h. About 2 weeks later, well-developed colonies of Wharton's Jelly mesenchymal stem cells (WJMSCs) appeared and were digested by 0.25% tyrisin (Gibco) and cultured on new plastic plates for passage.

WJMSCs at the third passage were collected and cultured in serum-free DMEM containing 0.5% bovine serum albumin (BSA) overnight. The conditioned medium was collected and centrifuged at 2000 g for 20 min to remove debris, and then ultracentrifuged at 100,000 g for 1 h at 4 °C. The precipitation was washed with serum-free M199 (Sigma-Aldrich, St. Louis, MO, USA) containing HEPES (25 mM; pH 7.4) followed by second ultracentrifugation. The obtained MVs were authenticated by transmission electron microscope (TEM) and flow cytometry (FCM). The mRNA expression of HGF were also determined by quantitative Real-Time PCR (qRT-PCR).

2.2. Lentivirus-mediated shRNA interference targeting HCF in MSC-MVs

Lentivirus vectors expressing three HGF short hairpin RNAs (shRNAs) were constructed using Mission Lentiviral Transduction Particles (Sigma-Aldrich) and lentivirus vectors carrying null shRNA were also packaged and used as negative control. Lentivirus packaging was performed in hWJMSC-MVs at the third passage using Lipofectamine 2000 (Invitrogen, Carlsbad, CA, USA) according to manufacturer's protocol. Transfection efficiency was confirmed by qRT-PCR.

2.3. Animals and experimental groups

Male Sprague-Dawley (SD) rats (SPF grade) weighing 180–200 g were kept at 22 ± 2 °C, with 12 h light/dark cycle and humidity of 55 ± 5%, which were purchased from

Laboratory Animal Centre of Shanghai Jiaotong University. Rats were randomly allocated to the following groups (n = 6 for each group): Control group: normal saline was instead of bleomycin (BLM).

ALI + vehicle group which were intratracheally administrated with BLM (4 mg/kg) and PBS as vehicle control.

ALI + MSC-MVs group which were intratracheally administrated with MSC-MVs 2 days after BLM (4 mg/kg) treatment.

ALI + Neg shRNA MSC-MVs group which were intratracheally administrated with negative siRNA MSC-MVs 2 days after BLM (4 mg/kg) treatment.

ALI + HGF shRNA MSC-MVs group which were intratracheally administrated with HGF shRNA MSC-MVs 2 days after BLM (4 mg/kg) treatment BLM (4 mg/kg).

After 48 h or 1 week, bronchoalveolar lavage fluid (BALF) samples and lungs were collected for the following experiments. Approval of the experimental protocols by the Animal Center of Shanghai Jiaotong University Affiliated First People's Hospital was obtained before conducting the experiments.

2.4. Cell culture and treatment

Rat type II alveolar epithelial cell line L2 and rat pulmonary microvascular endothelial cells (RPMVEC) purchased from American Type Culture Collection (ATCC, Manassas, VA, USA) were cultured in RPMI 1640 medium (Life Technologies) containing 10% FBS. The medium was changed every 48 h. Both cells of the third passage were used in the following experiments.

To examine the effect of MSC-MVs delivered HGF on BLM-induced ALI, the two cell lines were both divided into 5 subgroups: Control, BLM, BLM + MSC-MVs, BLM + Neg shRNA MSC-MVs and BLM + HGF shRNA MSC-MVs.

To further determine whether HGF mediated lung injury *via* PI3K-Akt-mTOR pathway, the two cell lines were randomized to 4 groups, namely, BLM, BLM + MSC-MVs, BLM + MSC-MVs + DMSO and BLM + MSC-MVs + LY294002.

2.5. Real time PCR

Total RNA was isolated using the RNApure Total RNAFast Extraction Kit (BioTeke, Beijing, China), and then reverse transcribed into complementary DNA (cDNA) using a reverse transcription kit (Takara, Beijing, China). Subsequently, primers for HGF were synthesized by Sangon Biotechnology (Shanghai, China). Finally, the mRNA expression of HGF was determined by qRT-PCR performing on7500 FAST real-time PCR System (Applied Biosystems, Carlsbad, CA, USA).

2.6. Measurement of total protein content in the BALF

Rats were euthanatized by inhalation of ether at the indicated time points. Bronchoalveolar lavage (BAL) was carried out by instilling 1 mL of 0.9% saline through the tracheal cannula, and BALF was centrifuged at 10, 000 g for 5 min. Supernatants were stored at −80 °C until assayed. Total protein concentration in BALF was measured to examine pulmonary permeability. BALF was mixed with Bio-Rad solution (Bio-Rad Laboratories, Richmond, CA, USA) and incubated at room temperature for 10 min. The absorbance of the fluid was then read at 595 nm on a spectrophotometer. The protein concentration was determined by comparison with the standard curve using bovine serum albumin.

2.7. Cell counts

For determination of total white blood cell (WBC), 1 mL of BALF was stained with Turk solution consisting of 1 mL glacial acetic acid, 1 mL of gentian violet solution, and 100 mL distilled water and counted using a Neubauer chamber.

BALF samples were centrifuged at 1,500 g for 10 min, and then the cell pellet were diluted in PBS, fixed in methanol and stained with a modified pappenheim stain (Merck, Darmstadt, Germany). Neutrophil quantification was achieved *via* light microscopy by two experienced and blinded members.

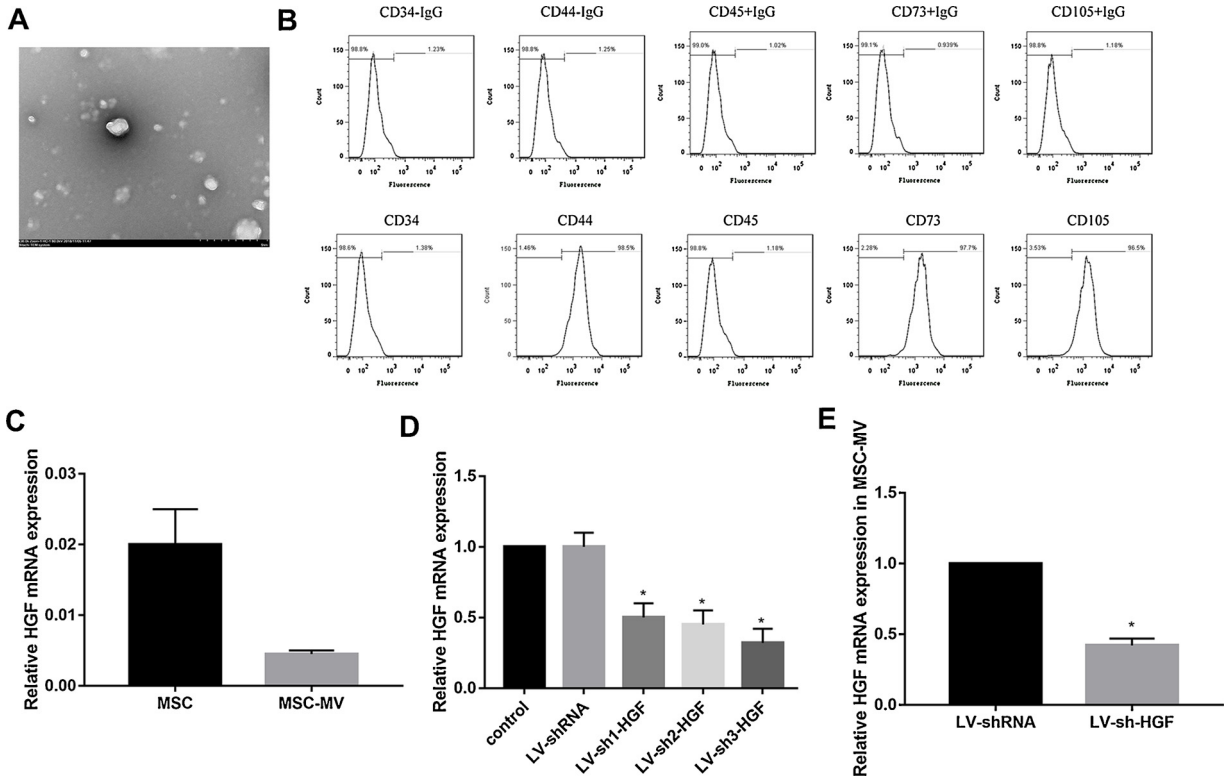

Fig. 1. Identification of MSC-MVs and HGF shRNA lentivirus transfection.
(A) Transmission and scanning electron microscopy performed on purified MSC-MVs indicated their spheroid morphology and confirmed their size. (B) Cell surface markers of MSC-MVs, including CD44, CD73, CD105, CD34 and CD45 were analyzed by flow cytometry. (C) The mRNA expression of HGF in MSCs and MSC-MVs determined by qRT-PCR. HGF mRNA expression in MSCs (D) transfected with LV-shRNA, LV-sh1-HGF, LV-sh2-HGF and LV-sh3-HGF and MSC-MVs (E) transfected with LV-shRNA and LV-sh3-HGF.
*P < 0.05 *vs.* LV-shRNA group. n = 3.

2.8. Enzyme-linked immunosorbent assay

The concentration of tumor necrosis factor (TNF)-α, interleukin-6 (IL-6) and HGF in BALF were assayed using ELISA kits (eBioscience, San Diego, CA, USA) following the manufacturer's protocol.

2.9. TUNEL assay

The apoptotic lung tissue cells were assessed by TUNEL assay using *in situ* Cell Death Detection Kit (Roche Applied Science, Mannheim, Germany). Paraformalde-fixed slices were treated with protease K (10 mmol/L) for 15 min and stained with TUNEL reaction mixture at 37 °C for 1 h. After rinsing the slides three times, slides were incubated in DAB substrate for 10 min at room temperature and analyzed under light microscopy (Olympus Co., Tokyo, Japan). The apoptotic cells were quantified by a pathologist based on 5 randomly selected areas (×400 magnification). The apoptosis index was defined as the number of apoptotic cells divided by the total number of lung tissue cells.

2.10. Histological examinations

Lung tissues were fixed in 4% paraformaldehyde, followed by dehydration in an ethanol gradient. After paraffin embedding, lung tissues were sectioned into 5-μm thickness slices and then was processed for H &E staining and Masson's trichrome staining using kits (Sigma-Aldrich).

2.11. Immunofluorescence

Lung specimens were frozen in optimal cutting temperature compound for sectioning using a cryostat. Tissue sections (8-μm thick) on glass slides were fixed in methanol at −20 °C for 10 min, rehydrated with PBS, and then incubated with 3% BSA in PBS for 10 min. Slides were incubated overnight with anti-AT1α and anti-CD31 in 1% BSA in PBS. Samples were treated with the secondary antibodies Alexa Fluor 488 IgG (1:500) for 1 h at room temperature. Incubation with primary antibodies was routinely omitted in control experiments. Slides were finally washed, mounted in VectaShield mounting medium, and observed and photographed on a Zeiss Axio Observer Z1 inverted fluorescent microscope (Carl Zeiss Microimaging GmbH, Jena, Germany).

2.12. Western blot

The lung tissues were processed for western blotting as described previously. Briefly, the specimens were resuspended in RIPA buffer (Life Technologies). Equal amounts (10 μg) of total protein were separated in 12% SDS-PAGE and then transferred onto the membranes. Membranes were incubated with 5% non-fat milk in TBST (10 mM Tris–HCl, pH 8.0, 150 mM NaCl, and 0.2% Tween-20) for 1 h at 20 °C, and then with the appropriate primary antibody in TBST, which was one of anti-c-Met (Abcam, Cambridge, UK), anti-phospho-c-Met (Abcam), anti-Akt (Cell Signaling Technology, Boston, MA, USA), anti-phospho-Akt (Cell Signaling Technology), anti-mTOR (Cell Signaling Technology), anti-phospho-mTOR (Cell Signaling Technology), anti-HGF (Abcam), cleaved-caspase-3 (Cell Signaling Technology), or anti-β-actin (Cell Signaling Technology) at a dilution of 1:1000 overnight at 4 °C. Blots were then incubated with the appropriate secondary antibody at 20 °C for 2 h and finally washed three times with TBST. Bands were visualized using the enhanced chemiluminescence reagent kit (Millipore, Bedford, MA, USA). Quantification was performed by optical density methods. Results were expressed as the density relative to β-actin.

2.13. Annexin V-FITC/PI apoptotic assay

L2 cells were collected and then washed with PBS. After fixed with ethyl alcohol at 4 °C for 2 h, the cells were suspended in PBS. Afterwards, cells were stained with annexin V-FITC and propidine iodide (PI) at 4 °C under darkness for 30 min after filtration and centrifugation. Finally, cells were recorded using flow cytometry (Beckman Coulter, Fullerton, CA, USA).

2.14. Statistical analysis

Continuous variables were expressed as mean ± standard deviation (SD) if normally distributed, and analyzed for statistical significance using one-way ANOVA. Significance was set at $P < 0.05$.

3. Results

3.1. HGF mRNA is substantially expressed in WJMSCs and MSC-MVs

In this study, MVs were isolated from the conditioned medium of WJMSCs derived from human umbilical cord. MSC-MVs were observed under a transmission electron microscope, indicating their spheroid morphology with approximately 200 nM in size (Fig. 1A). The MVs were then identified by detecting surface markers including CD34, CD73, CD105, CD34, and CD45. Flow cytometry analyses showed the presence of several molecules such as CD44, CD73 and CD105 but not CD34 and CD45 (Fig. 1B).

Using qRT-PCR, we confirmed that both MSCs and MSC-MVs expressed the mRNA of HGF (Fig. 1C). To determine the optimal LV-HGF-shRNA for MSCs transfection, we performed qRT-PCR of MSCs for all three LV-HGF shRNA candidates at 48 h posttransfection, and found that the mRNA levels of HGF were most decreased in LV-shRNA3-HGF transfected MSCs compared with negative shRNA group (Fig.1D). The findings from qRT-PCR also indicated that HGF mRNA expression was downregulated by 50% in the MVs isolated from the supernatant of HGF shRNA3 MSCs (Fig. 1E).

3.2. MSC-MVs ameliorated BLM-induced ALI via HGF

To the best of our knowledge, the amount of total protein in BALF was a vital indicator of pulmonary vascular permeability. Our data showed that the total protein content in BALF was significantly elevated following BLM administration, which were reduced after 48 h or 1 week treatment of MSC-MVs. However, compared with Neg shRNA MSC-MVs group, HGF shRNA MSC-MVs administration after 48 h or 1 week treatment markedly increased total protein in BALF (Figs. 2A and 3 A). BLM-challenged rats showed significantly increased BALF WBC and neutrophils compared with the control group, which was also decreased by MSC-MVs treatment, while HGF shRNA MSC-MVs administration at 48 h or 1 week post-injury resulted in an increase in the amount of WBC and neutrophils (Figs. 2B-2C and 3 B-3C). As shown in Figs. 2D and 3 D, ALI rats exhibited a markedly increased mRNA expression of proinflammatory cytokines (TNF-α and IL-6) in BALF, which was reversed by MSC-MVs at 48 h or 1 week treatment. Treatment with HGF shRNA MSC-MVs for 2 days or 7 days observably upregulated the expression of the aforementioned molecules. HGF concentration in BALF was significantly increased at 48 h after BLM stimulation. Administration of MSC-MVs for 2 days or a week further elevated HGF level in BALF. However, HGF shRNA MSC-MVs administration inhibited HGF level in BALF as compared to negative shRNA MSC-MVs group (Figs. 2E and 3 E).

Besides, lung tissue cell apoptosis was remarkably promoted in ALI rats, whereas MV administration for 48 h greatly inhibited cell apoptosis, however, HGF shRNA exerted pro-apoptotic effect on lung tissue cells (Fig. 2F). HE staining of lung tissues showed that intratracheal BLM resulted in inflammatory cell influx, alveolar wall thickness, pulmonary consolidation, and pulmonary hyaline membrane, suggesting a robust inflammatory response in the alveolus in ALI rats. Simultaneous administration of MSC-MVs or Neg shRNA MSC-MVs, significantly attenuated the histological injury. Therapeutic effect on injured lung was attenuated in HGF shRNA MSC-MV group compared with Neg shRNA MSC-MVs group (Fig. 3F). By Masson staining, we found that BLM treatment destroyed the alveolar space and caused pulmonary interstitial collagen hyperplasia and protein deposition. Impressively, 1 week treatment of MSC-MVs could somewhat ameliorate the degree of lung injury. However, the administration of HGF shRNA MSC-MVs led to an opposite effect (Fig. 3G).

In view of the close association of HGF with c-Met dependent PI3K/Akt/mTOR signaling pathways, we also determined the alteration of this signaling elicited by MVs in the *in vivo* experimental setting. Western blot analysis revealed that, MVs overturned the effect of ALI-induced rapid decrease of c-Met, Akt, and mTOR phosphorylation levels. Treatment of shRNA HGF MSC-MVs suppressed c-Met, Akt, and mTOR phosphorylation (Fig. 3H) since shRNA HGF MSC-MVs led to HGF knockdown in lung tissues (Fig. 3I), especially in alveolar epithelial cells and vascular endothelial cells (Fig. 3J). To verify that HGF expression was particularly reduced in alveolar epithelial cells and vascular endothelial cells in the lung tissues of rats from the "ALI + HGF shRNA MSC-MVs" group, we perform double immunofluorescence to co-localize HGF expression with alveolar epithelial markers (AT1α) or endothelial markers (CD31). The results showed that downregulation of AT1α and CD31 was observed in ALI + vehicle group. However, treatment of MSC-MVs led to significant increase of AT1α and CD31 expression in lung tissues, suggesting that MSC-MVs promoted the proliferation of alveolar epithelial cells and vascular endothelial cells. In addition, HGF was not expressed in lung tissues of Control and ALI + vehicle group. MSC-MVs increased HGF protein levels in lung tissues. Compared to Neg shRNA MSC-MVs group, the administration of HGF shRNA MSC-MVs reduced the expression of AT1α and CD31 in lung tissues, implying that MSC-MVs promoted the proliferation of alveolar epithelial cells and vascular endothelial cells *via* transferring HGF mRNA (Supplementary Fig. 1). Taken together, these findings revealed that MSC-MVs administration could effectively alleviate BLM-induced ALI *via* HGF in rats.

3.3. MSC-MVs inhibited alveolar epithelial cells and RPMVEC apoptosis induced by BLM through transferring HGF mRNA via PI3K-Akt-mTOR pathway

Disruption of the blood-air barrier, which is formed by alveolar epithelial cells and lung vascular endothelial cells, is a hallmark of ALI (Bärnthaler et al., 2017). As demonstrated by flow cytometry, MVs inhibited BLM-induced late apoptosis in alveolar epithelial cells and RPMVECs (Figs. 4 A and 5 A). In contrast, HGF shRNA MSC-MVs played a pro-apoptotic role *via* decreasing the mRNA expression of HGF (Figs. 4B and 5 B) as well as inhibiting PI3K-Akt-mTOR activation (Figs. 4C and 5 C). Then, a PI3K inhibitor LY294002 completely abrogated apoptosis inhibition induced by MVs-treated alveolar epithelial cells and RPMVECs (Figs. 4D and 5 D). Apoptosis was further confirmed by determining the protein levels of cleaved-caspase-3. Western blotting indicated that MSC-MVs inhibited BLM-induced caspase-3 upregulation in L2 cells (Supplementary Fig. 2A-B) and RPMVECs (Supplementary Fig. 2C-D), while shRNA-mediated HGF silencing in MSC-MVs or LY294002 treatment increased caspase-3 expression in L2 cells (Supplementary Fig. 2A-B) and RPMVECs (Supplementary Fig. 2C-D). Collectively, our data suggested that MSC-MVs suppressed BLM-induced apoptosis of alveolar epithelial cells and lung vascular endothelial cells by delivering HGF mRNA *via* PI3K-Akt-mTOR signaling pathway.

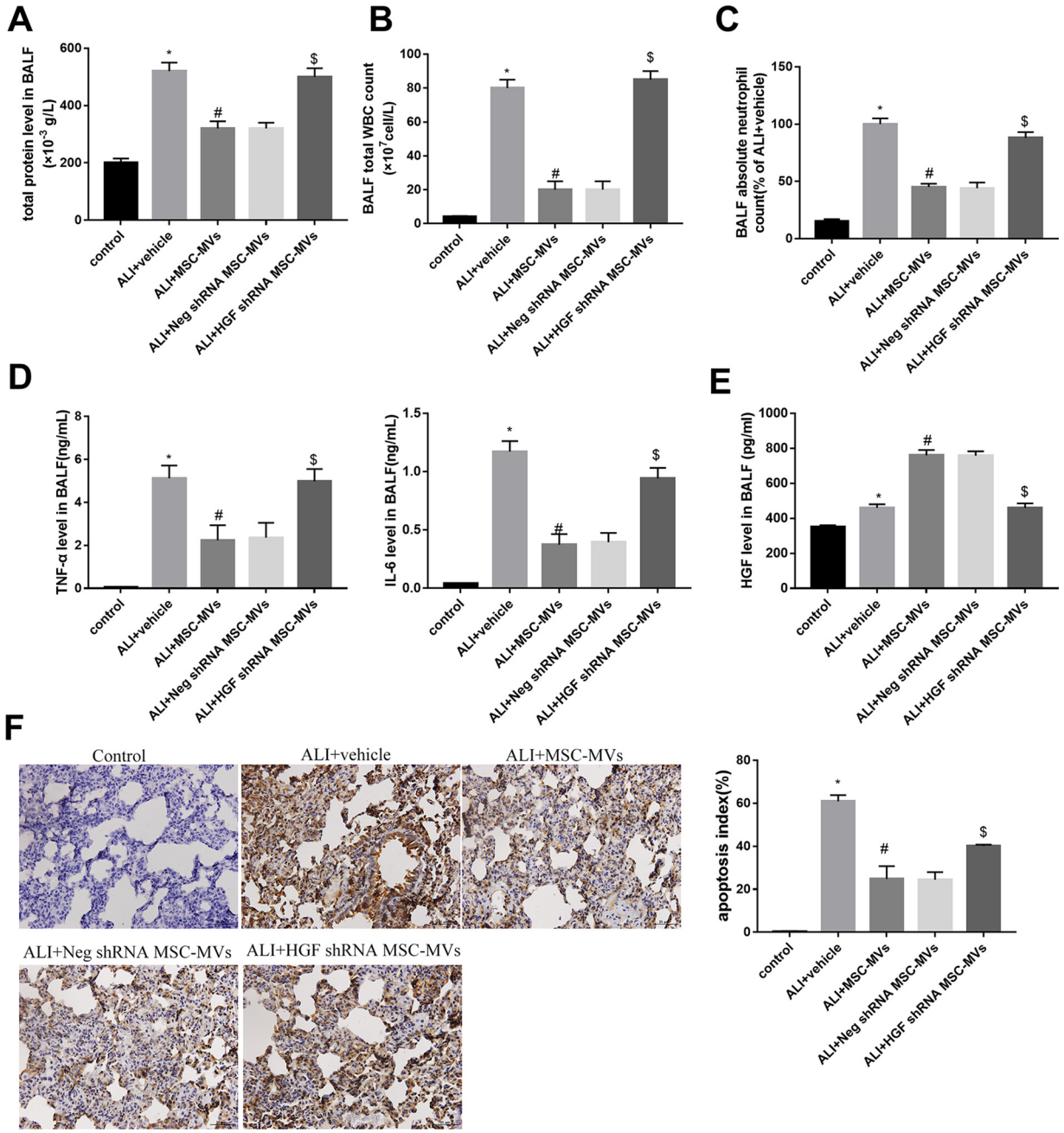

Fig. 2. Effect of 48 h MSC-MVs administration on BLM-induced ALI.
Total protein (A), WBC (B), neutrophils (C) and TNF-α, IL-6 (D), and HGF concentration (E) determined by ELISA in BALF and lung tissue cell apoptosis (F) using TUNEL assay in ALM rats following 48 h treatment of vehicle, MSC-MVs, Neg shRNA MSC-MVs or HGF shRNA MSC-MVs.
$^{*}P < 0.05$ *vs.* control group; $^{\#}P < 0.05$ *vs.* ALI + vehicle group; $^{\$}P < 0.05$ *vs.* ALI + HGF shRNA MSC-MVs. n = 6.

4. Discussion

In the present study, we established a rat model of BLM-induced ALI to investigate the therapeutic mechanism of MSC-MVs in the development of ALI. We found that intratracheal administration of WJMSCs-derived MVs ameliorated the lung inflammation induced by BLM in mice, including the influx of WBCs and neutrophils, and TNF-α and IL-6 secretion. Meanwhile, intratracheal administration of MSC-MVs restored the pulmonary fibrosis assessed by Masson's trichrome staining. Similar to MSCs, MSC-MVs expressed substantial quantity of HGF mRNA in rats. Furthermore, HGF shRNA MSC-MVs partly eliminated the beneficial effects of MVs on both lung inflammation and fibrosis, suggesting that the therapeutic effects of MSC-MVs appears to be partly mediated by HGF mRNA, with subsequently HGF protein expression. In L2 cells, a rat type II alveolar epithelial cell line MSC and in RPMVECs, MVs exerted anti-apoptotic effects *via* activating PI3K-Akt-mTOR signaling pathway.

Previous studies have demonstrated the therapeutic potential of WJMSCs in BLM-induced model of lung injury (Moodley et al., 2009). Our recent studies have demonstrated that WJMSCs mitigated AKI *via* rescuing the fibrotic lesions in an endocrine manner, thereby facilitating tubular cell resistance to apoptosis and cell proliferation (Du and Zhu, 2014; Tao et al., 2012). Gennai et al (Gennai et al., 2015) showed that MSC-MVs restored alveolar fluid clearance, decreased lung weight gain, and improved airway and hemodynamic parameters in an *ex vivo* lung perfusion model. A large quantity of evidence has revealed that

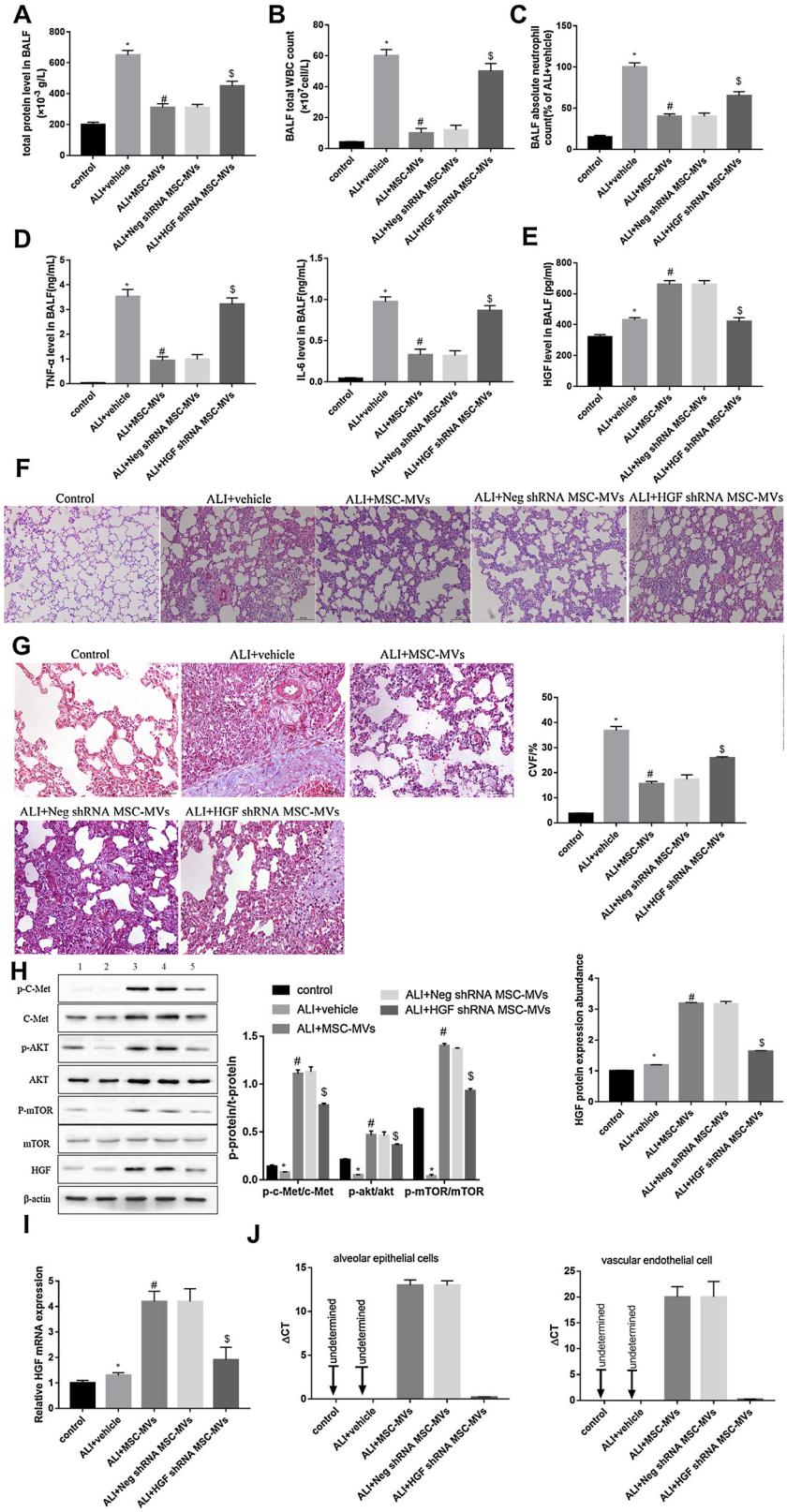

Fig. 3. Effect of 1 week MSC-MVs administration on BLM-induced ALI.

Total protein (A), WBC (B; 1: Control, 2: ALI + vehicle, 3: ALI + MSC-MVs, 4: ALI + Neg shRNA MSC-MVs, 5: ALI + HGF shRNA MSC-MVs), neutrophils (C) and TNF-α, IL-6 (D), and HGF concentration (E) in BALF; H&E (F) and Masson staining (G), the protein levels of c-Met, p-c-Met, Akt, p-Akt, mTOR, p-mTOR and HGF (H), the mRNA levels of HGF in lung tissues (I); the mRNA levels of HGF (J) in alveolar epithelial cells and vascular endothelial cells in ALI rats following 48 h treatment of vehicle, MSC-MVs, Neg shRNA MSC-MVs or HGF shRNA MSC-MVs.

$^{*}P < 0.05$ *vs.* control group; $^{\#}P < 0.05$ *vs.* ALI + vehicle group; $^{\$}P < 0.05$ *vs.* ALI + HGF shRNA MSC-MVs. n = 6.

MSC-MVs may transfer proteins/peptides, mRNA, microRNA, lipids, and/or organelles with reparative and anti-inflammatory properties to the injured tissues (Cha et al., 2018). Zhu et al (Ying-Gang et al., 2014) reported that MSC-MVs, through transferring keratinocyte growth factor (KGF) mRNA to injured sites, partly restored lung protein permeability and reduced inflammation in ALI mice induced by E. coli endotoxin. Tang et al (Tang et al., 2017) found that angiopoietin-1 (HGF) mRNA partly mediated the therapeutic effects of MSC MVs on ALI in mice induced by lipopolysaccharide (LPS). These results collectively suggested that KGF or HGF mRNA were not the exclusive way of contributing to the therapeutic benefit in ALI. Based on the finding of a substantial quantity of HGF mRNA within MSC MVs, we confirmed the

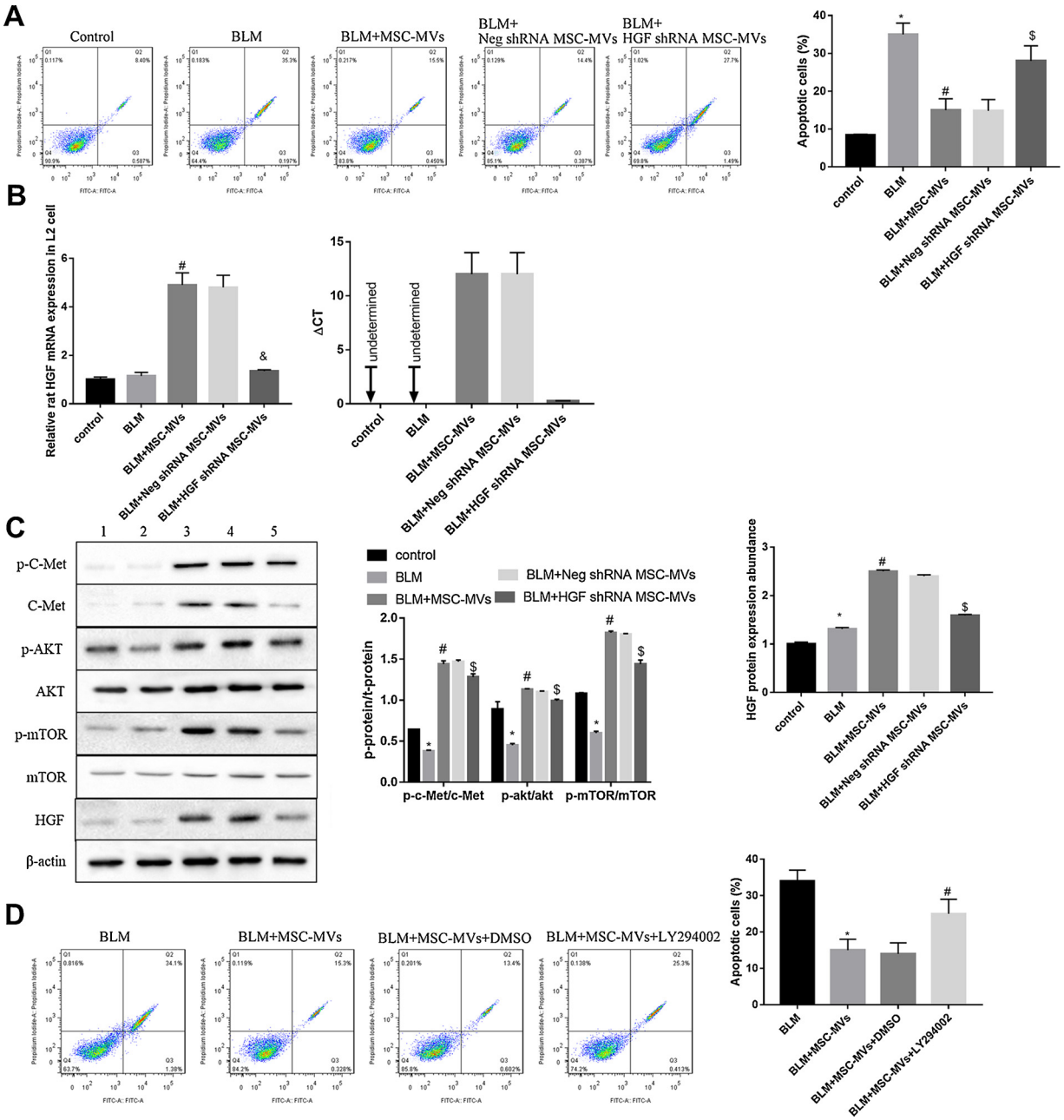

Fig. 4. Effect of MSC-MVs on apoptosis of alveolar epithelial cells induced by BLM Annexin V-FITC/PI apoptotic assay (A), HGF mRNA levels (B) and the protein levels of c-Met, p-c-Met, Akt, p-Akt, mTOR, p-mTOR and HGF (C) in rat type II alveolar epithelial cell line L2 in the groups of Control, BLM, BLM + MSC-MVs, BLM + Neg shRNA MSC-MVs, and BLM + HGF shRNA MSC-MVs; $^{*}P < 0.05$ *vs.* control group; $^{\#}P < 0.05$ *vs.* BLM group; $^{\$}P < 0.05$ *vs.* BLM + Neg shRNA MSC-MVs.

(D) Annexin V-FITC/PI apoptotic assay in rat type II alveolar epithelial cell line L2 in the groups of BLM, BLM + MSC-MVs, BLM + MSC-MVs + DMSO and BLM + MSC-MVs + LY294002. $^{*}P < 0.05$ *vs.* BLM group; $^{\#}P < 0.05$ *vs.* BLM + MSC-MVs + DMSO group. n = 3.

hypothesis that the therapeutic effects of MSC MVs in ALI were also partly mediated by HGF mRNA.

In our BLM-induced ALI model, MSC-MVs administration increased HGF protein level in BALF probably through transferring HGF mRNA to the injured alveolar epithelial cells and pulmonary vascular endothelial cells. Our previous researches have strongly implied the important role of HGF mRNA in therapeutic effects of MSC-MVs in ischemia-induced renal fibrosis, such as on releasing from G2/M cell cycle arrest *via* Erk1/2 signaling or contributing to tubular EMT delay (Chen et al., 2017; Du et al., 2013a,2013b). It was well documented that the pathophysiological process of ALI involves epithelial and endothelial cell perturbation and inflammatory cell influx leading to surfactant disruption, pulmonary edema, and atelectasis (Mason et al., 2002). HGF, originally identified as the most potent mitogen for mature parenchyma hepatocytes, has been reported to be involved in anti-apoptotic, anti-inflammatory, and tissue regeneration processes during tissue repair injury (Rong et al., 2018; Wang et al., 2018). Compelling evidence has delineated the important role for HGF in the protective effects mediated by MSCs in BLM-induced pulmonary fibrosis (Cahill et al., 2016). Several recent studies have shown that HGF secretion by MSCs was responsible for improving lung pathological injury through anti-oxidative anti-apoptotic and anti-inflammatory mechanisms (Chen et al., 2016b). HGF/PI3K-Akt-mTOR axis plays an essential role in EMT and angiogenesis in lung tissue cells (Chen et al., 2016a; Jiao et al., 2016).

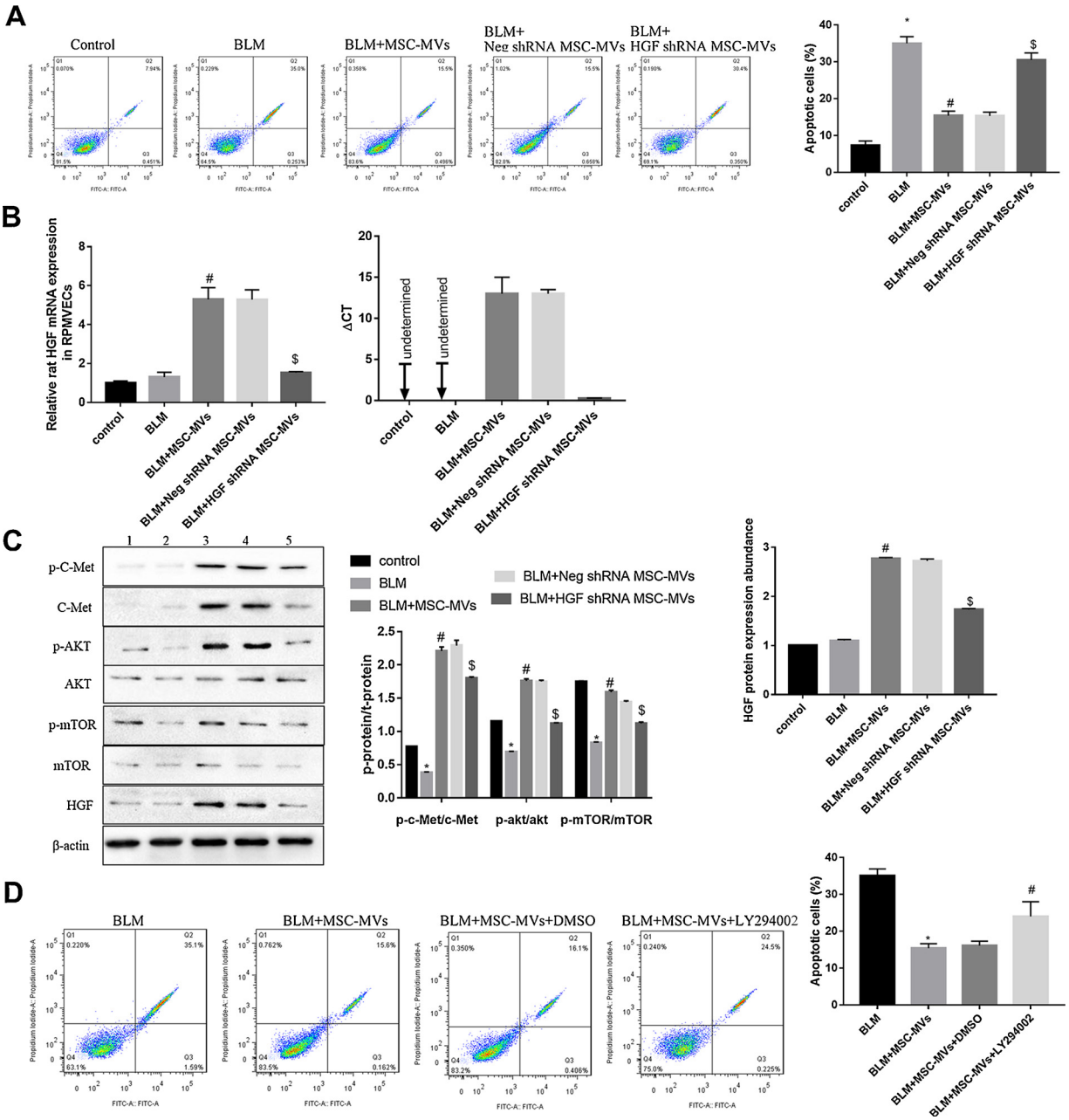

Fig. 5. Effect of MSC-MVs on RPMVEC apoptosis induced by BLM.
Annexin V-FITC/PI apoptotic assay (A), HGF mRNA levels (B) and the protein levels of c-Met, p-c-Met, Akt, p-Akt, mTOR, p-mTOR and HGF (C) in RPMVECs in the groups of Control, BLM, BLM + MSC-MVs, BLM + Neg shRNA MSC-MVs, and BLM + HGF shRNA MSC-MVs; $^{*}P < 0.05$ *vs.* control group; $^{\#}P < 0.05$ *vs.* BLM group; $^{\$}P < 0.05$ *vs.* BLM + Neg shRNA MSC-MVs.
(D) Annexin V-FITC/PI apoptotic assay in rat type II alveolar epithelial cell line L2 in the groups of BLM, BLM + MSC-MVs, BLM + MSC-MVs + DMSO and BLM + MSC-MVs + LY294002. $^{*}P < 0.05$ *vs.* BLM group; $^{\#}P < 0.05$ *vs.* BLM + MSC-MVs + DMSO group. n = 3.

In this study, we determined that PI3K inhibitor LY294002 abrogated the anti-apoptotic effect of MSC-MVs in rat type II alveolar epithelial cell line MSC and RPMVECs.

In summary, we now provided the first evidence revealing that HGF mRNA partly mediated the therapeutic effects of MSC-MVs on ALI in mice induced by BLM *via* PI3K-Akt-mTOR activation.

Conflict of interest

All the authors declare no conflict of interest.

Funding

This study is supported by grants from the Natural Science Research Program of the Education Department of Henan Province (17A360018) and the Basic Research Program of Science and Technology Department of Henan Province (132300410058).

Appendix A. Supplementary data

Supplementary material related to this article can be found, in the online version, at doi:https://doi.org/10.1016/j.biocel.2019.05.010.

References

Bärnthaler, T., Maric, J., Platzer, W., Konya, V., Theiler, A., Hasenöhrl, C., Gottschalk, B., Trautmann, S., Schreiber, Y., Graier, W.F., 2017. The role of PGE 2 in alveolar epithelial and lung microvascular endothelial crosstalk. Sci. Rep. 7 (1), 7923.

Biancone, L., Bruno, S., Deregibus, M.C., Tetta, C., Camussi, G., 2012. Therapeutic potential of mesenchymal stem cell-derived microvesicles. Nephrol. Dial. Transplant. 27 (8), 3037–3042.

Cahill, E.F., Kennelly, H., Carty, F., Mahon, B.P., English, K., 2016. Hepatocyte growth factor is required for mesenchymal stromal cell protection against bleomycin-induced pulmonary fibrosis. Stem Cells Transl. Med. 5 (10), 1307–1318.

Camussi, G., Deregibus, M.C., Bruno, S., Cantaluppi, V., Biancone, L., 2010. Exosomes/microvesicles as a mechanism of cell-to-cell communication. Kidney Int. 78 (9), 838–848.

Cha, J.M., Shin, E.K., Ji, H.S., Moon, G.J., Kim, E.H., Cho, Y.H., Park, H.D., Bae, H., Kim, J., Bang, O.Y., 2018. Efficient scalable production of therapeutic microvesicles derived from human mesenchymal stem cells. Sci. Rep. 8 (1).

Chan, M.C., Kuok, D.I., Leung, C.Y., Hui, K.P., Valkenburg, S.A., Lau, E.H., Nicholls, J.M., Fang, X., Guan, Y., Lee, J.W., Chan, R.W., Webster, R.G., Matthay, M.A., Peiris, J.S., 2016. Human mesenchymal stromal cells reduce influenza A H5N1-associated acute lung injury in vitro and in vivo. Proc. Natl. Acad. Sci. U.S.A. 113 (13), 3621–3626.

Chen, Q.Y., Jiao, D.M., Wu, Y.Q., Chen, J., Wang, J., Tang, X.L., Mou, H., Hu, H.Z., Song, J., Yan, J., Wu, L.J., Chen, J., Wang, Z., 2016a. MiR-206 inhibits HGF-induced epithelial-mesenchymal transition and angiogenesis in non-small cell lung cancer via c-Met /PI3k/Akt/mTOR pathway. Oncotarget 7 (14), 18247–18261.

Chen, S., Chen, X., Wu, X., Wei, S., Han, W., Lin, J., Kang, M., Chen, L., 2016b. Hepatocyte growth factor -modified mesenchymal stem cells improve ischemia reperfusion-induced acute lung injury in rats. Gene Ther. 24 (1).

Chen, W., Yan, Y., Song, C., Ding, Y., Du, T., 2017. Microvesicles derived from human Wharton's Jellymesenchymal stem cells ameliorate ischemia-reperfusion-induced renal fibrosis by releasing from G2/M cell cycle arrest. Biochem. J. 474, 4207–4218 BCJ20170682.

Du, T., Zou, X., Cheng, J., Wu, S., Zhong, L., Ju, G., Zhu, J., Liu, G., Zhu, Y., Xia, S., 2013a. Human Wharton's jelly-derived mesenchymal stromal cells reduce renal fibrosis through induction of native and foreign hepatocyte growth factor synthesis in injured tubular epithelial cells. Stem Cell Res. Ther. 4 (3), 59.

Du, T., Zou, X., Cheng, J., Wu, S., Zhong, L., Ju, G., Zhu, J., Liu, G., Zhu, Y., Xia, S., 2013b. Human Wharton's jelly-derived mesenchymal stromal cells reduce renal fibrosis through induction of native and foreign hepatocyte growth factor synthesis in injured tubular epithelial cells. Stem Cell Res. Ther. 4 (3), 59.

Du, T., Zhu, Y.J., 2014. The regulation of inflammatory mediators in acute kidney injury via exogenous mesenchymal stem cells. Mediators Inflamm. 2014 (6), 261697.

Gennai, S., Monsel, A., Hao, Q., Park, J., Matthay, M.A., Lee, J.W., 2015. Microvesicles Derived From Human Mesenchymal Stem Cells Restore Alveolar Fluid Clearance in Human Lungs Rejected for Transplantation. Am. J. Transplant. 15 (9), 2404–2412.

Han, Y., Luo, Y., Wang, Y., Chen, Y., Li, M., Jiang, Y., 2016. Hepatocyte growth factor increases the invasive potential of PC-3 human prostate cancer cells via an ERK/MAPK and Zeb-1 signaling pathway. Oncol. Lett. 11 (1), 753–759.

Ho, M.S., Mei, S.H., Stewart, D.J., 2015. The immunomodulatory and therapeutic effects of mesenchymal stromal cells for acute lung injury and sepsis. J. Cell. Physiol. 230 (11), 2606–2617.

Jiao, D., Wang, J., Lu, W., Tang, X., Chen, J., Mou, H., Chen, Q.Y., 2016. Curcumin inhibited HGF-induced EMT and angiogenesis through regulating c-Met dependent PI3K/Akt/mTOR signaling pathways in lung cancer. Mol. Ther. Oncolytics 3, 16018.

Ju, G.Q., Cheng, J., Zhong, L., Wu, S., Zou, X.Y., Zhang, G.Y., Gu, D., Miao, S., Zhu, Y.J., Sun, J., Du, T., 2015. Microvesicles derived from human umbilical cord mesenchymal stem cells facilitate tubular epithelial cell dedifferentiation and growth via hepatocyte growth factor induction. PLoS One 10 (3), e0121534.

Mason, R.J., Gao, B., Pan, T., Jiang, X., Eckart, M., Neben, S., 2002. Role of keratinocyte growth factor in regulating lipogenesis in alveolar type II cells: a gene-profiling approach. Chest 121 (3), 77S.

Meng, L., Li, L., Lu, S., Li, K., Su, Z., Wang, Y., Fan, X., Li, X., Zhao, G., 2018. The protective effect of dexmedetomidine on LPS-induced acute lung injury through the HMGB1-mediated TLR4/NF-kappaB and PI3K/Akt/mTOR pathways. Mol. Immunol. 94, 7–17.

Monsel, A., Zhu, Y.G., Gudapati, V., Lim, H., Lee, J.W., 2016. Mesenchymal stem cell derived secretome and extracellular vesicles for acute lung injury and other inflammatory lung diseases. Expert Opin. Biol. Ther. 16 (7), 859–871.

Moodley, Y., Atienza, D., Manuelpillai, U., Samuel, C.S., Tchongue, J., Ilancheran, S., Boyd, R., Trounson, A., 2009. Human umbilical cord mesenchymal stem cells reduce fibrosis of bleomycin-induced lung injury. Am. J. Pathol. 175 (1), 303–313.

Ratajczak, M.Z., Kucia, M., Jadczyk, T., Greco, N.J., Wojakowski, W., Tendera, M., Ratajczak, J., 2012. Pivotal role of paracrine effects in stem cell therapies in regenerative medicine: can we translate stem cell-secreted paracrine factors and microvesicles into better therapeutic strategies? Leukemia 26 (6), 1166–1173.

Rong, S., Wang, X., Wang, Y., Wu, H., Zhou, X., Wang, Z., Wang, Y., Xue, C., Li, B., Gao, D., 2018. Anti-inflammatory activities of hepatocyte growth factor in post-ischemic heart failure. Acta Pharmacol. Sin.

Squillaro, T., Peluso, G., Galderisi, U., 2016. Clinical trials with mesenchymal stem cells: an update. Cell Transplant. 25 (5), 829.

Tang, X.D., Shi, L., Monsel, A., Li, X.Y., Zhu, H.L., Zhu, Y.G., Qu, J.M., 2017. Mesenchymal stem cell microvesicles attenuate acute lung injury in mice partly mediated by Ang-1 mRNA. Stem Cells 35 (7), 1849–1859.

Tao, D., Liang, Z., Xin-Feng, Z., Jiang, Z., Ying-Jian, Z., Guo-Hua, L., 2012. The alleviation of acute and chronic kidney injury by human Wharton's jelly-derived mesenchymal stromal cells triggered by ischemia-reperfusion injury via an endocrine mechanism. Cytotherapy 14 (10), 1215–1227.

Wang, L.S., Wang, H., Zhang, Q.L., Yang, Z.J., Kong, F.X., Wu, C.T., 2018. Hepatocyte growth factor gene therapy for ischemic diseases. Hum. Gene Ther. 413–423.

Ying-Gang, Z., Xiao-Mei, F., Jason, A., Xiao-Hui, F., Qi, H., Antoine, M., Jie-Ming, Q., Matthay, M.A., Lee, J.W., 2014. Human mesenchymal stem cell microvesicles for treatment of Escherichia coli endotoxin-induced acute lung injury in mice. Stem Cells 32 (1), 116–125.

Yuan, W., Li, L., Hu, Y., Li, W., Guo, Z., Huang, W., 2016. Inhibition of acute lung injury by TNFR-Fc through regulation of an inflammation-oxidative stress pathway. PLoS One 11 (3), e0151672.